

# Synthesis of Novel 6-(4-Substituted piperazine-1-yl)-9-( $\beta$ -D-ribofuranosyl)purine Derivatives, Which Lead to Senescence-Induced Cell Death in Liver Cancer Cells

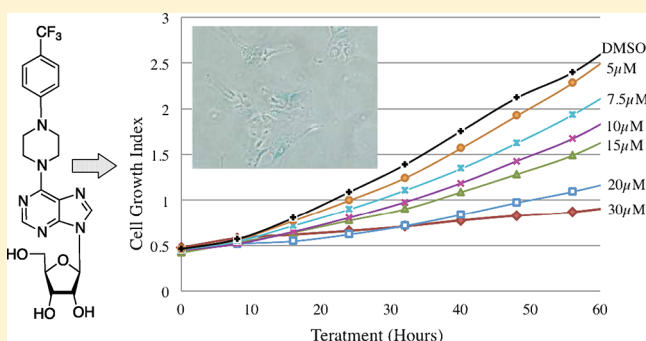
Meral Tuncbilek,<sup>\*,†</sup> Ebru Bilget Guven,<sup>‡</sup> Tugce Onder,<sup>†</sup> and Rengul Cetin Atalay<sup>\*,‡,§</sup>

<sup>†</sup>Department of Pharmaceutical Chemistry, Faculty of Pharmacy, Ankara University, 06100 Ankara, Turkey

<sup>‡</sup>Department of Molecular Biology and Genetics, Bilkent University, 06800 Ankara, Turkey

<sup>§</sup>Bilkent University Genetics and Biotechnology Research Center (BilGen), Bilkent University, 06800, Ankara, Turkey

**ABSTRACT:** Novel purine ribonucleoside analogues (9–13) containing a 4-substituted piperazine in the substituent at N<sup>6</sup> were synthesized and evaluated for their cytotoxicity on Huh7, HepG2, FOCUS, Mahlavu liver, MCF7 breast, and HCT116 colon carcinoma cell lines. The purine nucleoside analogues were analyzed initially by an anticancer drug-screening method based on a sulforhodamine B assay. Two nucleoside derivatives with promising cytotoxic activities (11 and 12) were further analyzed on the hepatoma cells. The N<sup>6</sup>-(4-Trifluoromethylphenyl)piperazine analogue 11 displayed the best antitumor activity, with IC<sub>50</sub> values between 5.2 and 9.2  $\mu$ M. Similar to previously described nucleoside analogues, compound 11 also interferes with cellular ATP reserves, possibly through influencing cellular kinase activities. Furthermore, the novel nucleoside analogue 11 was shown to induce senescence-associated cell death, as demonstrated by the SA $\beta$ -gal assay. The senescence-dependent cytotoxic effect of 11 was also confirmed through phosphorylation of the Rb protein by p15<sup>INK4b</sup> overexpression in the presence of this compound.



## INTRODUCTION

Nucleobase analogues and nucleoside analogues are significant drugs used in chemotherapy for the treatment of solid tumors and hematological malignancies.<sup>1</sup> These groups of compounds are considered antimetabolites because nucleobases and nucleosides are the metabolic precursors of nucleotides. Nucleotides and their derivatives are involved in a large number of cellular processes, including cell growth and division, and for this reason nucleobase and nucleoside analogues have been exploited as anticancer agents.<sup>2</sup> Initially, nucleobase analogues such as fluorinated pyrimidines were investigated as antimetabolite chemotherapeutic agents on cancer cells. Later, pyrimidine analogues Ara-C and Gemcitabine were used in cancer therapy.<sup>3</sup> Success with pyrimidine nucleoside analogues in cancer therapy led to the discovery of purine nucleoside analogues. For more than six decades, 6-mercaptopurine and 6-thioguanine have been used as inhibitors of nucleic acid metabolism in pediatric acute lymphoblastic leukemia.<sup>4</sup> Currently, the purine nucleoside analogues fludarabine, cladribine, and pentostatin are used for treating hematological malignancies.<sup>5</sup> The synthetic nucleoside analogues fludarabine and cladribine are synthesized into the dATP analogues, and the natural substance pentostatin leads to an increase in the dATP levels in the cell. Nucleoside analogues create an imbalance in the cellular dNTP reserve by inhibiting the ribonucleotide reductase enzyme, which in turn leads to

impaired DNA synthesis.<sup>6</sup> For this reason, nucleoside analogues often cause apoptosis-induced cell death.<sup>3</sup> Recently, expression levels of ribonucleotide reductase subunits have been proposed as molecular markers for nucleoside analogue-induced cell death in cancer therapy response; nevertheless, it was previously shown that reduced ribonucleotide reductase and altered dNTP pools have been associated with cellular senescence in diploid fibroblasts.<sup>7–9</sup> Hence, nucleoside analogues too, may induce senescence-associated cell death.

Apoptosis and necrosis are the most-studied chemotherapeutic-induced cell death mechanisms. However, in the past decade, senescence, autophagy, and mitotic catastrophe have been shown to be induced by cytotoxic agents.<sup>10</sup> Senescence-associated growth arrest is a significant cellular event in tumor development and progression. Initially, replicative senescence was reported to be due to telomere shortening during replication.<sup>11</sup> Later, Serrano et al. showed that premature senescence was associated with cancer.<sup>12</sup> Studies on the molecular analysis of senescence in cancer revealed oncogene-induced senescence (OIS) and tumor-suppressor-dependent senescence (PICS).<sup>13,14</sup> Therefore, senescence-induced cell death through pro-senescence therapy is currently the target of small-molecule inhibitors.<sup>14</sup>

Received: October 31, 2011

Published: March 12, 2012

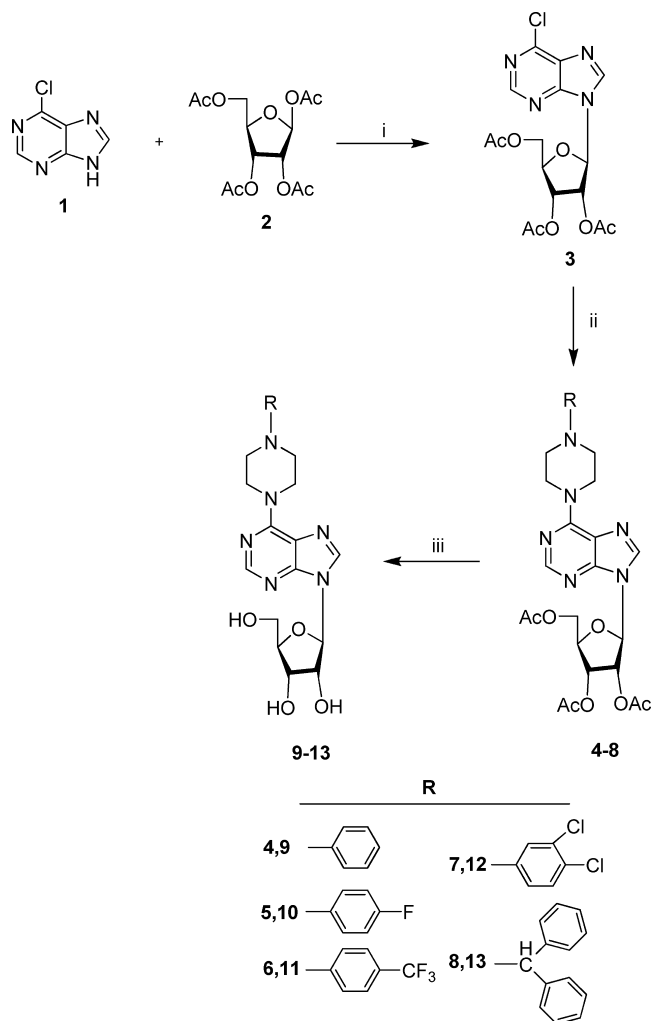
Recently, studies focusing on evading senescence in murine premalignant hepatocytes have revealed a mechanism called senescence surveillance during hepatocarcinogenesis.<sup>15</sup> Furthermore, replacement of the tumor suppressor p53 in murine liver cancer models has led to senescence and therefore to regression of these tumors. Primary liver cancer, hepatocellular carcinoma (HCC), is the fourth most common cause of cancer mortality and the third most common malignancy in human cancers. Chronic liver injury is due to viral diseases, exposure to chemicals, and other environmental or autoimmune conditions that are the risk factors for HCC. These factors induce an acquired tolerance to genotoxic stress, but ultimately a cancerous state that does not respond to the cellular death mechanisms.<sup>16</sup> Recently, Sorafenib, a multikinase inhibitor, was approved by the FDA and the EU for hepatocellular carcinoma treatment.<sup>17</sup> Sorafenib prolongs median survival and the time to progression by nearly three months in patients with advanced hepatocellular carcinoma. Therefore, there is a need for new liver-cancer-specific drugs based on the molecular mechanisms involved in liver carcinogenesis. In this study, we synthesized novel purine ribonucleoside analogues (9–13) containing a 4-substituted piperazine in the substituent at N<sup>6</sup> as putative cytotoxic agents. The newly obtained compounds were then characterized for their anticancer senescence-inducing activity in liver cancer cells.

## RESULTS AND DISCUSSION

**Chemistry.** The 6-(4-substituted piperazine-1-yl)-9-( $\beta$ -D-ribofuranosyl)purine derivatives (9–13) were synthesized as shown in Scheme 1. 6-Chloropurine (1) was condensed with the sugar 1,2,3,5-tetra-*O*-acetyl- $\beta$ -D-ribofuranose (2) under microwave irradiation (30 min) to obtain 6-chloro-9-(2,3,5-tri-*O*-acetyl- $\beta$ -D-ribofuranosyl)-9*H*-purine (3) as a yellowish foam in good yield of 75.7%. This reaction gave significantly higher yields than the previously published method.<sup>18</sup> Displacement of the 6-chloro was accomplished by nucleophilic substitution with appropriate N-substituted piperazines. Removal of the acetyl-protecting groups was performed with NaOMe in MeOH to produce nucleosides 9–13.

**Biological Evaluation and Discussion.** The newly synthesized compounds 9–13 were first evaluated for their antitumor activities against human liver (Huh7), colon (HCT116), and breast (MCF7) carcinoma cell lines (Figure 1A). The IC<sub>50</sub> values were in micromolar concentrations with N<sup>6</sup>-(substituted phenyl)piperazine purine nucleoside derivatives (Figure 1A and Table 1). We then tested the cytotoxic effect of these molecules on additional hepatocellular carcinoma (HCC) cell lines: HepG2, Mahlavu, and FOCUS (Figure 1B). We observed strong cell growth inhibition in the presence of the novel nucleosides 11 and 12. Time-dependent IC<sub>50</sub> values for each molecule were also calculated in comparison with the nucleobase analogue 5-fluorouracil (5-FU) and DNA topoisomerase inhibitor camptothecin (CPT) (Table 1). N<sup>6</sup>-(4-Trifluoromethylphenyl)piperazine derivative 11 displayed the best cytotoxic activity, with IC<sub>50</sub> values of 5.2–9.2  $\mu$ M (Table 1). The (3,4-dichlorophenyl)piperazine derivative 12 was also very active (IC<sub>50</sub> values in the range of 5.5–9.7  $\mu$ M) against all tested cell lines. When there was a larger substituent at the 4-position of piperazine moiety (diphenylmethyl group, 13), cytotoxic activity was decreased. On the other hand, compound 9, which has no substitution at the phenyl ring, did not show any significant cytotoxic activity; the compound 10, with 4-fluorophenyl, had some cytotoxicity (Table 1). Nucleosides 11

Scheme 1<sup>a</sup>



<sup>a</sup>Reagents: (i) silica gel 60, EtOAc, microwave irradiation; (ii) the appropriate piperazine, TEA, EtOH; (iii) NaOMe, MeOH.

and 12 demonstrated significant cytotoxicity for all the cell lines tested. When we compared their IC<sub>50</sub> values with the known cell growth inhibitors CPT and 5-FU, we observed that our compounds 11 and 12 had showed lower values in micromolar concentrations. Compounds 11 and 12 had a better cytotoxic activity on Huh7 cells (7.8 and 7.1 vs 30.7  $\mu$ M for 5-FU).

Considering the cytotoxic activity of our novel nucleosides 9–13 on hepatoma cell lines, we further analyzed the cellular activity of the most potent inhibitor (11) on these cell lines as a promising candidate anticancer agent.

**Real-Time Cellular Response of Hepatocellular Carcinoma Cells with Compound 11 Treatment.** Real-time cell electronic sensing (RT-CES) was used to evaluate compound 11's mediated cytotoxicity on Huh7, HepG2, Mahlavu, and FOCUS hepatoma cells in triplicate (Figure 2). Real-time dynamic monitoring of the electrode impedance indicates a cell index (CI) that correlates with cell growth. Compound 11 triggered a time- and dose-dependent decrease in CI cell growth indexes in all hepatoma cells (Figure 2). A cell growth index with 30–5  $\mu$ M of compound 11 treatment clearly demonstrates the potent inhibitor action of compound 11, which correlates with our initial observation with the NCI-SRB assay. The PTEN-deficient cell line Mahlavu was the least

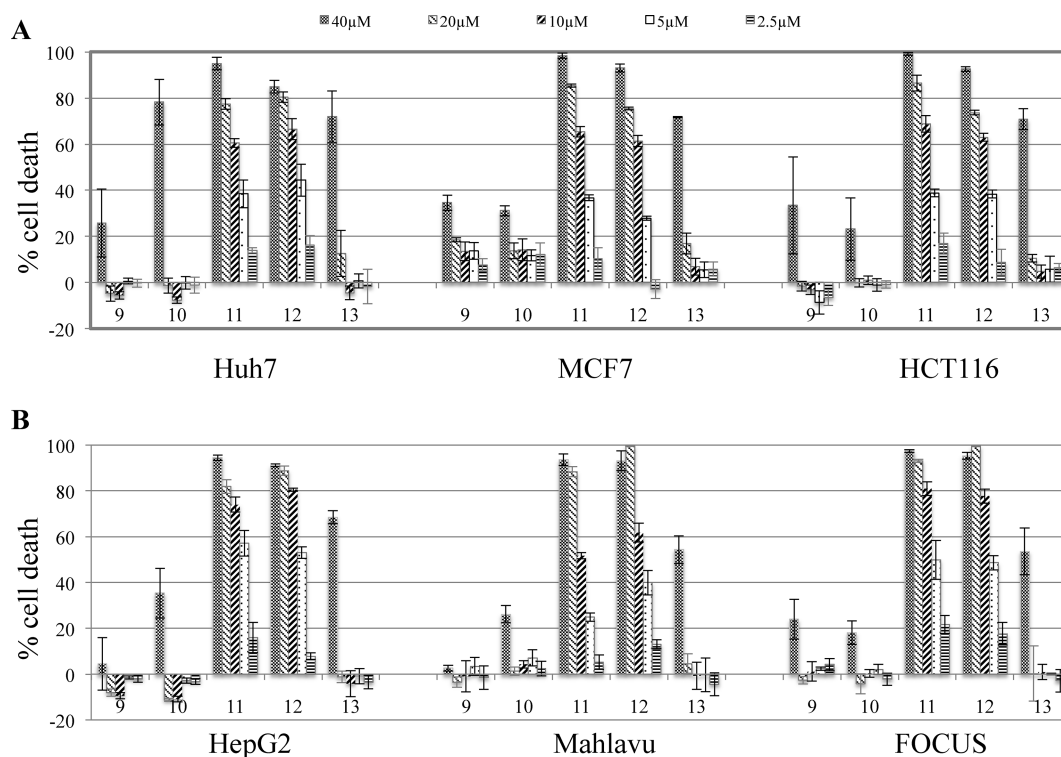


**Figure 1.** Percent cell death in the presence of compounds 9–13. Huh7, HCT116, MCF7 (A) and HepG2, Mahlavu and FOCUS (B) cells were inoculated in 96-well plates. All molecules and their DMSO controls were administered to the cells in triplicate with five different concentrations: 40, 20, 10, 5, and 2.5  $\mu\text{M}$ . After 72 h of incubation, SRB assays were generated and the cell death percentages were calculated in comparison with DMSO-treated wells.

**Table 1.**  $\text{IC}_{50}$  Values in  $\mu\text{M}$  Concentrations for 9–13 with 72 h of Treatment<sup>a</sup>

	9	10	11	12	13	5-FU	CPT
Huh7	>100	49.7	7.8	7.1	44.4	30.7	<0.1
HepG2	>100	>100	5.7	6.1	63.5	5.0	<0.1
Mahlavu	>100	>100	9.2	7.0	92.7	10.0	<0.1
FOCUS	>100	>100	5.2	5.5	>100	7.6	<0.1
HCT116	>100	>100	6.7	8.4	48.5	6.0	<0.1
MCF7	>100	>100	7.5	9.7	40.1	3.5	<0.1

<sup>a</sup> $\text{IC}_{50}$  values were calculated from the cell growth inhibition percentages obtained with five different concentrations.

affected by **11** (Mahlavu cells have a hyperactive PI3K/Akt pathway due to PTEN deficiency).<sup>19</sup> Higher nucleoside–**11** concentrations were needed for the cytotoxicity on Mahlavu cells. This observation indicated that compound–**11** might be a putative kinase–protein interfering molecule. For that reason, we tested a nontargeted broad-spectrum kinase assay with the aim of detecting cellular ATP levels affected by the presence of **11**.

**Nucleoside Analogue 11 Possesses Kinase-Inhibitor Potential.** With the aim of elucidating the possible kinase-interfering activity of **11**, we used a luminescent ATP-detection assay. Luminescence correlates with the amount of ATP in the milieu, therefore an increase in the luminescence might indicate the presence of a protein kinase inhibitor. Because of their established kinase-inhibition potentials, we used staurosporine (STS), a multikinase inhibitor, and the nucleoside analogue 5'-deoxy-5'-methylthioadenosine (MeSAdo) as positive controls for the experiment. Huh7 cells were incubated with  $\text{IC}_{50}$  and  $\text{IC}_{100}$  values of **11** (Table 1), 5  $\mu\text{M}$  MeSAdo, and 0.5  $\mu\text{M}$  STS

for 72 h. A luminescent ATP-detection assay was then achieved. The luminescence (measured as relative light units (*rlu*)) indicated a dose-dependent ATP amount in the presence of **11** similar with MeSAdo (Figure 3) with the same cell count. High *rlu* values obtained with the STS-treated Huh7 cells are consistent with both the principle of the assay and the molecular mechanism of STS as a multikinase inhibitor.

**The Cytotoxic Activity of 11 Is Neither Apoptosis nor Necrosis.** We then characterized the cytotoxic pathways involved in the molecular action of **11**. The apoptotic pathway activation indicator Poly-ADP-ribosyl-polymerase (PARP)'s protein cleavage was assessed on Huh7, HepG2, Mahlavu, and FOCUS cells in the presence of **11**. For each cell line, **11** was used as its cell-line-specific  $\text{IC}_{50}$  value for 72 h (Table 1). The endogenous PARP protein has an atomic mass of 113 kDa. During apoptosis, PARP is cleaved into 89 kDa and 24 kDa fragments, and when the cytotoxic effect is due to necrosis, the cleaved PARP is detected as a 50 kDa fragment band in Western blot analysis.<sup>20</sup> Seventy-two hours of treatment with **11** did not induce cleavage of the PARP protein in all treated liver cancer cell lines (data not shown). This cleavage analysis demonstrated that the cytotoxic activity of **11** was neither apoptosis nor necrosis.

**Compound 11 Induces Cellular Senescence.** Replicative senescence has long been characterized as proliferative arrest that occurs in normal cells after a limited number of population doublings. Recently, premature senescence has been associated with cancer cells. INK4a and INK4b proteins inhibit CyclinD1/CCDK4, leading to pRB activation and therefore induction of senescence. For this reason, higher expression of these proteins is among the premature senescence markers (in addition to

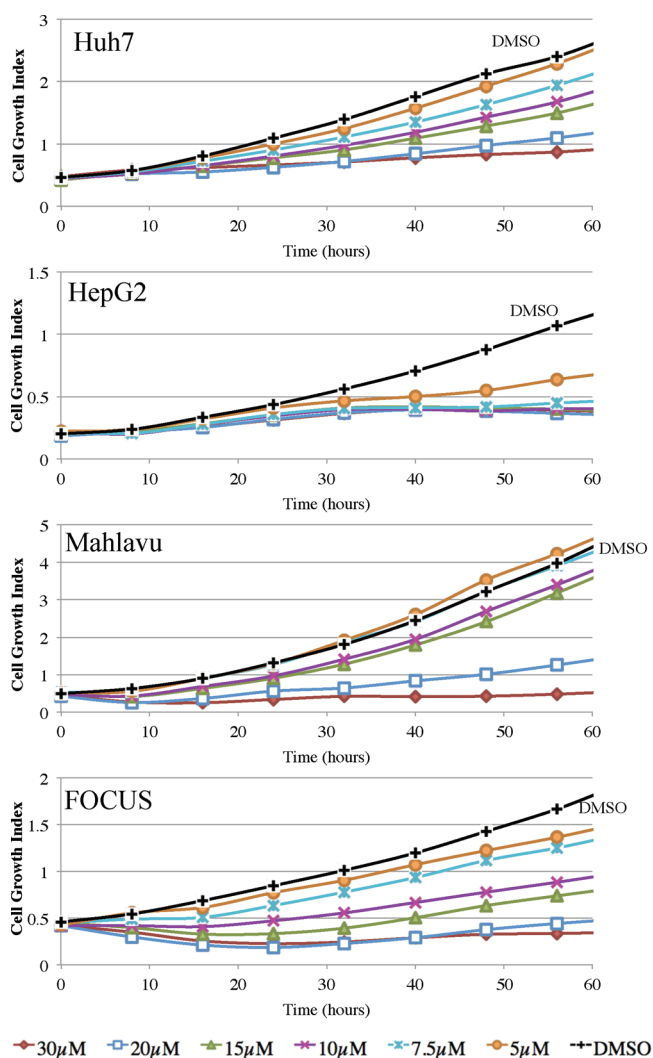


**Figure 2.** Real-time cell growth of Huh7, HepG2, Mahlavu, and FOCUS cells in the presence of compound **11**. Cells were inoculated in triplicate in E-plates. The cell growth index was monitored every 30 min in the presence of the different concentrations of compound **11** (30  $\mu\text{M}$ , red; 20  $\mu\text{M}$ , blue; 15  $\mu\text{M}$ , green; 10  $\mu\text{M}$ , magenta; 7.5  $\mu\text{M}$ , cyan; 5  $\mu\text{M}$ , coral; DMSO control, black).

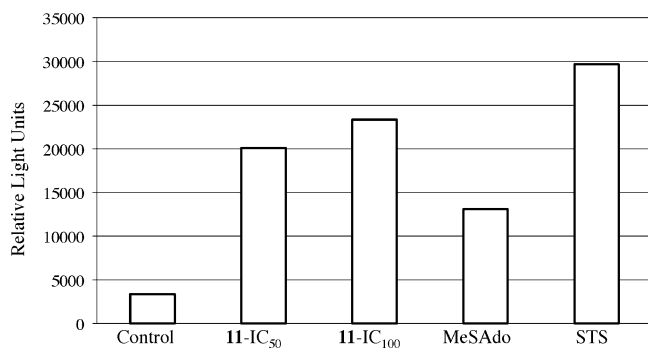


**Figure 3.** Whole cell protein kinase activity in the presence of **11**. Huh7 cells were incubated with  $\text{IC}_{50}$  and  $\text{IC}_{100}$  values of **11** (Table 1), staurosporine (STS, 0.5  $\mu\text{M}$ ), MeSAdo (0.5  $\mu\text{M}$ ), and their corresponding DMSO controls for 72 h. Then, using the Kinase-Glo assay kit, 80000 were cells tested for their ATP content by chemoluminescence.

senescence-associated  $\beta$ -galactosidase (SA $\beta$ -gal) activity at pH 6.0 due to increased lysosomal activity).

With the aim of identifying the possible senescence-involved cytotoxic activity of **11**, we performed a SA $\beta$ -gal assay and BrdU incorporation assays in parallel. Huh7 cells were plated in six-well plates on coverslips at low density for the logarithmic phase growth. The next day, Huh7 cells were treated with **11** at its  $\text{IC}_{50}$  and  $\text{IC}_{100}$  values both for three or six days. Doxorubicin (25 ng/mL) was used as a positive control for senescence-inducing agent, and DMSO was used as the negative control. Twenty-four hours prior to the end of the incubation with the compound, BrdU was administered to test its incorporation into the cellular DNA. The large blue-stained senescent (SA $\beta$ -gal-assay-positive) cells were negative for BrdU incorporation for compound **11** and doxorubicin (Figure 4A,B) when

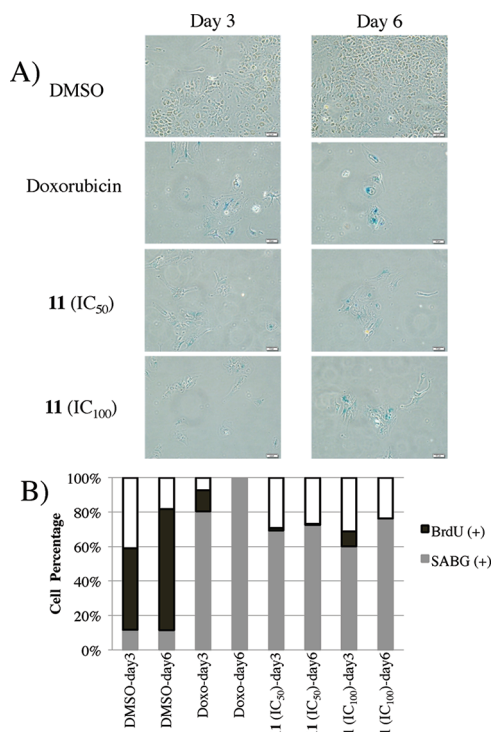


**Figure 4.** SA $\beta$ -gal and BrdU assays with compound **11**. Huh7 cells were plated on coverslips in six-well plates (5000 cells/well). (A) Huh7 cells were incubated with  $\text{IC}_{50}$  and  $\text{IC}_{100}$  values of **11**, doxorubicin, and DMSO only controls for three and six days. Doxorubicin was used as a positive control at its senescence-inducing dose (25 ng/mL). BrdU (30  $\mu\text{M}$ ) was administered to the cells 24 h prior to the end of three and six days of incubation. (B) Cells were counted and the percent distribution between SA $\beta$ -gal and BrdU positive was presented.

compared to the DMSO control. However, BrdU-positive proliferating cells were marked visible in DMSO-treated wells only.

**Compound 11-Induced Senescence Is Associated with the Induction of p15<sup>INK4b</sup> and a Decrease in Rb Phosphorylation.** In addition to testing for the most widely used and accepted marker of senescent cells (an increase in SA $\beta$ -gal activity), we tested another senescence-associated marker (p15<sup>INK4b</sup> levels) in **11**-treated Huh7 cells. Huh7 cells were treated in the presence of  $\text{IC}_{50}$  and  $\text{IC}_{100}$  concentrations of **11** both for three and six days, then Western blot analysis was realized. Indeed, we observed an increase in the protein

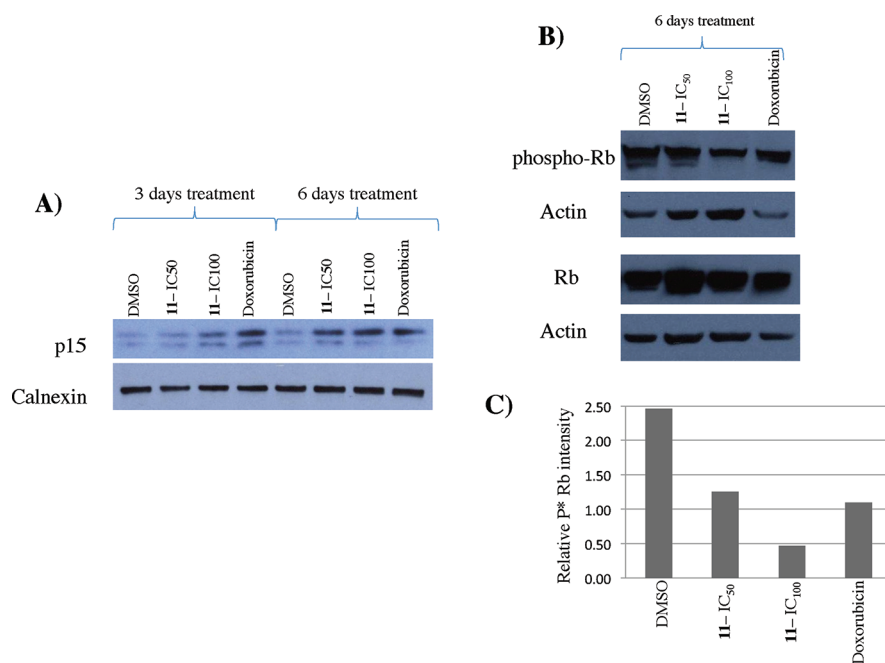


**Figure 5.** Senescence-associated proteins p15<sup>INK4b</sup> and pRb proteins in the presence **11**. Huh7 cells were treated with IC<sub>50</sub> and IC<sub>100</sub> values of **11**, doxorubicin, and DMSO for three and six days. Doxorubicin was used as a positive control at its senescence-inducing dose (25 ng/mL). (A) p15<sup>INK4b</sup> protein expression by Western blotting after three and six days of treatment in comparison with positive control doxorubicin and negative control DMSO. Treatment of Huh7 cells with **11** induced the accumulation of p15<sup>INK4b</sup> in a dose- and time-dependent manner. (B) Rb activity is detected with anti-Rb and antiphospho-Rb antibodies. (C) Comparative Rb phosphorylation levels confirmed senescence-induced cytotoxicity by compound **11**. Calnexin protein was used as an equal loading control.

expression levels of p15<sup>INK4b</sup> in a dose- and time-dependent manner (Figure 5A). Next, we determined the downstream effect of p15<sup>INK4b</sup> on the phosphorylation of the Rb protein. It is known that p15<sup>INK4b</sup> activates the Rb protein by inhibiting CyclinD1/CCDK4CD and therefore inhibits the phosphorylation of Rb. An observed decrease in the phosphorylated-form of the Rb protein correlates with the **11**-induced accumulation of p15<sup>INK4b</sup> (Figure 5A,B). This observation thus also confirmed the senescence-induced cytotoxic activity of compound **11**.

## CONCLUSION

We synthesized a novel group of nucleoside analogues (*N*<sup>6</sup>-substituted piperazine derivatives) as putative anticancer agents. We identified their cytotoxic activity and determined the minimum required concentration for their action. Two molecules, **11** and **12**, were promising as candidate chemotherapeutic agents and had IC<sub>50</sub> values less than 10 μM. We selected the most active compound (**11**) to pursue further experiments on with the aim of analyzing its molecular cytotoxic action on hepatoma cells. Our results indicated that the novel candidate chemotherapeutic agent **11** induces senescence-associated cell death through the inhibition of some kinase proteins (Figures 3 and 4). In addition our analysis with p15<sup>INK4b</sup> protein levels in **11**-treated cells indicates that the target kinases could be upstream of this protein; this must be further investigated in detail.

Recent studies on the involvement of senescence-associated cell death in cancer have established the concept *stress* or *aberrant signaling-induced* senescence (STASIS), which is telomere independent.<sup>21</sup> Reprogramming senescence in cancer cells was extensively discussed as one of the hallmarks of cancer.<sup>22</sup> Targeting replicative immortality and inducing

senescence has also been proposed for mechanism-based drug discovery. For this reason, induction of irreversible cell cycle arrest by senescence with novel candidate chemotherapeutic agents has become an important strategy against cancer.

## EXPERIMENTAL SECTION

**Chemistry.** Melting points were recorded with a capillary melting point apparatus (Electrothermal 9100) and are uncorrected. NMR spectra were recorded on a VARIAN Mercury 400 FT-NMR spectrometer (400 for <sup>1</sup>H, 100.6 MHz for <sup>13</sup>C). TMS was used as internal standard for the <sup>1</sup>H and <sup>13</sup>C NMR spectra; values are given in δ (ppm) and *J* values are in Hz. High resolution mass spectra data (HRMS) were collected in-house using a Waters LCT Premier XE mass spectrometer (high sensitivity orthogonal acceleration time-of-flight instrument) operating in ESI (+) method, also coupled with an AQUITY Ultra Performance liquid chromatography system (Waters Corporation, Milford, MA, USA). All compounds were of >95% purity. Elemental analyses (C, H, N) were determined on a Leco CHNS 932 instrument and gave values within ±0.4% of the theoretical values. Microwave reactions were carried out using a domestic microwave oven (White Westinghouse SG-KM97VL, 50 Hz, 1400 W). Column chromatography was accomplished on silica gel 60 (40–63 mm particle size). The chemical reagents used in synthesis were purchased from E. Merck, Fluka, Sigma, and Aldrich.

**6-Chloro-9-(2,3,5-tri-*O*-acetyl-β-*D*-ribofuranosyl)-9*H*-purine (3).** 6-Chloropurine (**1**) (154 mg, 1 mmol) and 1,2,3,5-tetra-*O*-acetyl-β-*D*-ribofuranose (**2**) were dissolved in EtOAc, and then 500 mg of silica gel 60 (200–400 mesh) was added. The mixture was concentrated in vacuo, and the dry residue was irradiated for 30 min in a White Westinghouse SG-KM97VL domestic microwave oven (50 Hz, 1400 W). The residue was purified by flash chromatography on silica gel (EtOAc–hexane, 3:1) to yield **3** as yellowish viscous oil (312.3 mg, 75.72%). <sup>1</sup>H NMR (CDCl<sub>3</sub>) δ 2.07 (s, 3H, OAc), 2.10 (s, 3H, OAc), 2.14 (s, 3H, OAc), 4.34–4.48 (m, 3H, H-4', H-5'), 5.63 (t, *J* = 5.2 Hz, 1H, H-3'), 5.93 (t, *J* = 5.6 Hz, 1H, H-2'), 6.21 (d, *J* = 5.2 Hz, 1H, H-1'), 8.28 (s, 1H, H-8), 8.76 (s, 1H, H-2). <sup>13</sup>C NMR (CDCl<sub>3</sub>) δ

20.59, 20.74, 20.97 (3 × CH<sub>3</sub>), 63.09 (CH<sub>2</sub>-5'), 70.67 (CH-4'), 73.32 (CH-3'), 80.74 (CH-2'), 87.08 (CH-1'), 132.57 (C-5), 143.79 (C-8), 151.44 (C-6), 151.87 (C-4), 152.54 (C-2), 169.56, 169.78, 170.48 (3 × CO). HRMS (ESI+) *m/z* calcd for C<sub>16</sub>H<sub>18</sub>ClN<sub>4</sub>O<sub>7</sub> (M + H)<sup>+</sup> 413.0864, found 413.0859. Anal. Calcd for C<sub>16</sub>H<sub>17</sub>ClN<sub>4</sub>O<sub>7</sub>·0.6EtOAc: C, 47.46; H, 4.71; N, 12.03. Found C, 47.84; H, 4.59; N, 11.89.

**General Procedure for the Synthesis of Compounds 4–8.** 6-Chloro-9-(2,3,5-tri-*O*-acetyl-β-*D*-ribofuranosyl)-9*H*-purine (3) was dissolved in 10 mL of absolute EtOH, and then 1-substituted piperazines and (Et)<sub>3</sub>N (3 equiv) were added. The mixture was refluxed for 3–8 h. The reaction mixture was concentrated in vacuo, and the residue was purified by column chromatography.

**6-(4-Phenylpiperazine-1-yl)-9-(2,3,5-tri-*O*-acetyl-β-*D*-ribofuranosyl)-9*H*-purine (4).** The compound was prepared from (3) (174.4 mg, 0.4 mmol) and 1-phenylpiperazine (0.13 mL, 0.8 mmol) at reflux for 4 h according to the general procedure and was purified by column chromatography (EtOAc–hexane, 1:1) to yield 4 (209 mg; 92%); mp 62–64 °C. <sup>1</sup>H NMR (CDCl<sub>3</sub>) δ 2.08 (s, 3H, OAc), 2.14 (s, 6H, OAc), 3.32 (t, 4H, piperazine CH<sub>2</sub>), 4.34–4.50 (m, 7H, H-4', H-5', piperazine CH<sub>2</sub>), 5.66 (t, *J* = 5.6 Hz, 1H, H-3'), 5.91 (t, *J* = 5.2 Hz, 1H, H-2'), 6.22 (d, *J* = 5.6 Hz, 1H, H-1'), 6.91 (t, 1H, *J* = 7.2 Hz, H-4 in phenyl), 6.98 (d, 2H, *J* = 7.6 Hz, H-2,6 in phenyl), 7.30 (t, 2H, *J* = 7.6 Hz, H-3,5 in phenyl), 7.92 (s, 1H, H-8), 8.37 (s, 1H, H-2). <sup>13</sup>C NMR (CDCl<sub>3</sub>) δ 20.65, 20.78, 21.03 (3 × CH<sub>3</sub>), 45.24, 49.85 (CH<sub>2</sub> in piperazine), 63.41 (CH<sub>2</sub>-5'), 70.95 (CH-3'), 73.32 (CH-2'), 80.40 (CH-4'), 86.12 (CH-1'), 116.78, 120.63, 129.45 (C in phenyl), 136.71 (C-5), 150.99 (C-8), 151.37 (C-6), 152.98 (C-2), 154.01 (C-4), 169.63, 169.85, 170.57 (3 × CO). HRMS (ESI+) *m/z* calcd for C<sub>26</sub>H<sub>31</sub>N<sub>6</sub>O<sub>7</sub> (M + H)<sup>+</sup> 539.2254, found 539.2253. Anal. Calcd for C<sub>26</sub>H<sub>30</sub>N<sub>6</sub>O<sub>7</sub>·0.5H<sub>2</sub>O: C, 57.03; H, 5.70; N, 15.34. Found C, 57.35; H, 5.58; N, 14.97.

**6-[4-(4-Fluorophenyl)piperazine-1-yl]-9-(2,3,5-tri-*O*-acetyl-β-*D*-ribofuranosyl)-9*H*-purine (5).** The compound was prepared from (3) (140.1 mg, 0.3 mmol) and 1-(4-fluorophenyl)piperazine (61.1 mg, 0.3 mmol) at reflux for 7 h according to the general procedure and was purified by column chromatography (EtOAc–hexane, 1:1) to yield 5 (151 mg; 80.3%); mp 57–59 °C. <sup>1</sup>H NMR (CDCl<sub>3</sub>) δ 2.08 (s, 3H, OAc), 2.14 (s, 6H, OAc), 3.22 (t, 4H, piperazine CH<sub>2</sub>), 4.35–4.47 (m, 6H, H-4', H-5', piperazine CH<sub>2</sub>), 5.66 (t, *J* = 4.8 Hz, 1H, H-3'), 5.91 (t, *J* = 5.2 Hz, 1H, H-2'), 6.22 (d, *J* = 5.6 Hz, 1H, H-1'), 6.91–7.02 (m, 4H, H-2,3,5,6 in phenyl), 7.92 (s, 1H, H-8), 8.37 (s, 1H, H-2). <sup>13</sup>C NMR (CDCl<sub>3</sub>) δ 20.64, 20.77, 21.02 (3 × CH<sub>3</sub>), 45.29, 50.88 (CH<sub>2</sub> in piperazine), 63.39 (CH<sub>2</sub>-5'), 70.92 (CH-3'), 73.32 (CH-2'), 80.39 (CH-4'), 86.16 (CH-1'), 115.77, 115.99, 118.67 (2), 120.63 (C in phenyl), 136.75 (C-5), 148.02 (C-8), 150.99 (C-6), 152.95 (C-2), 153.98 (C-4), 169.62, 169.84, 170.56 (3 × CO). HRMS (ESI+) *m/z* calcd for C<sub>26</sub>H<sub>30</sub>FN<sub>6</sub>O<sub>7</sub> (M + H)<sup>+</sup> 557.2160, found 557.2163. Anal. Calcd for C<sub>26</sub>H<sub>29</sub>FN<sub>6</sub>O<sub>7</sub>·1.3EtOAc: C, 55.84; H, 5.91; N, 12.52. Found C, 56.10; H, 5.87; N, 12.14.

**6-[4-(4-Trifluoromethylphenyl)piperazine-1-yl]-9-(2,3,5-tri-*O*-acetyl-β-*D*-ribofuranosyl)-9*H*-purine (6).** The compound was prepared from (3) (92.8 mg, 0.23 mmol) and 1-(α,α,α-trifluoro-*p*-tolyl)piperazine (52.1 mg, 0.23 mmol) at reflux for 2.5 h according to the general procedure and was purified by column chromatography (EtOAc–hexane, 1:1) to yield 6 (106.4 mg; 78.23%); mp 68–70 °C. <sup>1</sup>H NMR (DMSO-*d*<sub>6</sub>) δ 2.04 (d, 6H, OAc), 2.13 (s, 3H, OAc), 3.45 (br s, 4H, piperazine CH<sub>2</sub>), 4.25–4.43 (m, 7H, H-4', H-5', piperazine CH<sub>2</sub>), 5.63 (t, 1H, H-3'), 6.03 (t, 1H, H-2'), 6.26 (d, *J* = 5.6 Hz, 1H, H-1'), 6.13 (d, *J*<sub>o</sub> = 8.8 Hz, 2H, H-2,6 in phenyl), 7.54 (d, *J*<sub>o</sub> = 8.4 Hz, 2H, H-3,5 in phenyl), 8.33 (s, 1H, H-8), 8.46 (s, 1H, H-2). <sup>13</sup>C NMR (DMSO-*d*<sub>6</sub>) δ 20.87, 21.03, 21.17 (3 × CH<sub>3</sub>), 44.50, 47.61 (CH<sub>2</sub> in piperazine), 63.47 (CH<sub>2</sub>-5'), 70.73 (CH-3'), 72.58 (CH-2'), 80.11 (CH-4'), 86.24 (CH-1'), 115.05, 118.78 (q), 120.23, 124.29 (C in phenyl), 126.87 (q) (CF<sub>3</sub>), 139.91 (C-5), 150.93 (C-8), 152.89 (C-6), 153.76 (C-2), 153.81 (C-4), 169.96, 170.14, 170.72 (3 × CO). HRMS (ESI+) *m/z* calcd for C<sub>27</sub>H<sub>30</sub>F<sub>3</sub>N<sub>6</sub>O<sub>7</sub> (M + H)<sup>+</sup> 607.2128, found 607.2115. Anal. Calcd for C<sub>27</sub>H<sub>29</sub>F<sub>3</sub>N<sub>6</sub>O<sub>7</sub>·0.3EtOAc: C, 53.51; H, 5.00; N, 13.28. Found C, 53.88; H, 5.04; N, 13.03.

**6-[4-(3,4-Dichlorophenyl)piperazine-1-yl]-9-(2,3,5-tri-*O*-acetyl-β-*D*-ribofuranosyl)-9*H*-purine (7).** The compound was prepared from

(3) (241.5 mg, 0.58 mmol) and 1-(3,4-dichlorophenyl)piperazine (135.1 mg, 0.58 mmol) at reflux for 8 h according to the general procedure and was purified by column chromatography (EtOAc–hexane, 1:1) to yield 7 (166.2 mg; 46.69%); mp 67–69 °C. <sup>1</sup>H NMR (CDCl<sub>3</sub>) δ 2.08 (s, 3H, OAc), 2.15 (s, 6H, OAc), 3.29 (t, 4H, piperazine CH<sub>2</sub>), 4.34–4.48 (m, 7H, H-4', H-5', piperazine CH<sub>2</sub>), 5.67 (t, *J* = 4.8 Hz, 1H, H-3'), 5.92 (t, *J* = 5.2 Hz, 1H, H-2'), 6.22 (d, *J* = 5.6 Hz, 1H, H-1'), 6.79 (dd, *J*<sub>o</sub> = 8.8 Hz, *J*<sub>m</sub> = 2.8 Hz, 1H, H-6 in phenyl), 7.0 (d, *J*<sub>m</sub> = 2.8 Hz, 1H, H-2 in phenyl), 7.29 (d, *J*<sub>o</sub> = 9.2 Hz, 1H, H-5 in phenyl), 7.93 (s, 1H, H-8), 8.37 (s, 1H, H-2). <sup>13</sup>C NMR (CDCl<sub>3</sub>) δ 20.64, 20.77, 21.02 (3 × CH<sub>3</sub>), 44.94, 49.21 (CH<sub>2</sub> in piperazine), 63.37 (CH<sub>2</sub>-5'), 70.91 (CH-3'), 73.33 (CH-2'), 80.39 (CH-4'), 86.23 (CH-1'), 115.92 (CH in phenyl), 117.86 (CH in phenyl), 120.66 (CH in phenyl), 122.98 (C in phenyl), 130.76 (C in phenyl), 133.09 (C in phenyl), 136.91 (C-5), 150.76 (C-8), 150.99 (C-6), 152.92 (C-2), 153.91 (C-4), 169.62, 169.83, 170.55 (3 × CO). HRMS (ESI+) *m/z* calcd for C<sub>26</sub>H<sub>28</sub>Cl<sub>2</sub>N<sub>6</sub>O<sub>7</sub> (M + H)<sup>+</sup> 607.1475, found 607.1475. Anal. Calcd for C<sub>26</sub>H<sub>28</sub>Cl<sub>2</sub>N<sub>6</sub>O<sub>7</sub>·0.2EtOAc: C, 51.50; H, 4.77; N, 13.44. Found C, 51.43; H, 4.65; N, 13.08.

**6-(4-(Diphenylmethyl)piperazine-1-yl)-9-(2,3,5-tri-*O*-acetyl-β-*D*-ribofuranosyl)-9*H*-purine (8).** The compound was prepared from (3) (312 mg, 0.7 mmol) and 1-(diphenylmethyl)piperazine (190.9 mg, 0.7 mmol) at reflux for 5 h according to the general procedure and was purified by column chromatography (EtOAc–hexane, 1:1) to yield 8 (166.8 mg; 35.1%); mp 81–83 °C. <sup>1</sup>H NMR (CDCl<sub>3</sub>) δ 2.06 (s, 3H, OAc), 2.12 (s, 3H, OAc), 2.13 (s, 3H, OAc), 2.52 (t, 4H, piperazine CH<sub>2</sub>), 4.19–4.44 (m, 8H, CH, H-4', H-5', piperazine CH<sub>2</sub>), 5.63 (t, *J* = 4.8 Hz, 1H, H-3'), 5.87 (t, *J* = 5.2 Hz, 1H, H-2'), 6.20 (d, *J* = 5.2 Hz, 1H, H-1'), 7.19 (t, 2H, *J*<sub>o</sub> = 7.6 Hz, H-4 in phenyl), 7.29 (t, 4H, *J*<sub>o</sub> = 7.6 Hz, H-3,5 in phenyl), 7.44 (d, 4H, *J*<sub>o</sub> = 7.2 Hz, H-2,6 in phenyl), 7.84 (s, 1H, H-8), 8.30 (s, 1H, H-2). <sup>13</sup>C NMR (CDCl<sub>3</sub>) δ 20.65, 20.78, 21.02 (3 × CH<sub>3</sub>), 45.46 (CH<sub>2</sub> in piperazine), 52.26 (CH<sub>2</sub> in piperazine), 63.39 (CH), 70.93 (CH<sub>2</sub>-5'), 73.30 (CH-3'), 76.35 (CH-2'), 80.34 (CH-4'), 85.96 (CH-1'), 120.52 (CH in phenyl), 127.31 (CH in phenyl), 128.19 (CH in phenyl), 128.78 (C in phenyl), 136.32 (C-5), 142.47 (C-8), 150.88 (C-6), 152.99 (C-2), 154.03 (C-4), 169.61, 169.85, 170.57 (3 × CO). HRMS (ESI+) *m/z* calcd for C<sub>33</sub>H<sub>37</sub>N<sub>6</sub>O<sub>7</sub> (M + H)<sup>+</sup> 629.2724, found 629.2719. Anal. Calcd for C<sub>33</sub>H<sub>36</sub>N<sub>6</sub>O<sub>7</sub>·0.7H<sub>2</sub>O: C, 61.80; H, 5.87; N, 13.10. Found C, 61.57; H, 5.89; N, 13.07.

**General Procedure for the Deacetylation of the Protected Nucleosides 9–13.** The protected nucleosides (4–8) were dissolved in 10 mL of absolute MeOH, and then NaOMe (30% in MeOH) (2 equiv) was added and stirred at room temperature for 1–12 h. The reaction mixture was concentrated in vacuo. The residue was dissolved with CH<sub>2</sub>Cl<sub>2</sub>:MeOH and purified by column chromatography.

**6-(4-Phenylpiperazine-1-yl)-9-(β-*D*-ribofuranosyl)-9*H*-purine (9).** The compound was prepared from (4) (209.1 mg, 0.388 mmol) at room temperature for 1 h according to general procedure and was purified by column chromatography (EtOAc–hexane, 3:1) to yield 9 (27 mg; 16.3%); mp 99–100 °C. <sup>1</sup>H NMR (DMSO-*d*<sub>6</sub>) δ 3.26 (t, 4H, piperazine CH<sub>2</sub>), 3.53–3.70 and 3.65–3.73 (2m, 2H, CH<sub>2</sub>-5'), 3.96–4.16 (m, 2H, H-2',3'), 4.38 (br s, 4H, piperazine CH<sub>2</sub>), 4.58 (q, 1H, H-4'), 5.21 (d, 1H, 3'-OH), 5.33 (t, 1H, 5'-OH), 5.48 (d, 1H, 2'-OH), 5.93 (d, 1H, 1'-H), 6.81 (t, 1H, *J* = 7.2 Hz, H-4 in phenyl), 7.0 (d, 2H, *J* = 8.4 Hz, H-2,6 in phenyl), 7.24 (t, 2H, *J* = 8.4 Hz, H-3,5 in phenyl), 8.28 (s, 1H, H-8), 8.45 (s, 1H, H-2). <sup>13</sup>C NMR (DMSO-*d*<sub>6</sub>) δ 49.15 (CH<sub>2</sub> in piperazine), 62.14 (CH<sub>2</sub>-5'), 71.13 (CH-3'), 74.20 (CH-2'), 86.42 (CH-4'), 88.44 (CH-1'), 116.51, 119.97, 120.32, 129.65 (C in phenyl), 139.66 (C-5), 150.99 (C-8), 151.61 (C-6), 152.47 (C-2), 153.81 (C-4). HRMS (ESI+) *m/z* calcd for C<sub>20</sub>H<sub>25</sub>N<sub>6</sub>O<sub>4</sub> (M + H)<sup>+</sup> 413.1937, found 413.1938. Anal. Calcd for C<sub>20</sub>H<sub>24</sub>N<sub>6</sub>O<sub>4</sub>·1.2H<sub>2</sub>O: C, 55.34; H, 6.13; N, 19.36. Found C, 54.97; H, 6.07; N, 18.98.

**6-[4-(4-Fluorophenyl)piperazine-1-yl]-9-(β-*D*-ribofuranosyl)-9*H*-purine (10).** The compound was prepared from (5) (151 mg, 0.27 mmol) at room temperature for 5 h according to the general procedure and was purified by column chromatography (EtOAc–hexane, 4:1 and then EtOAc) to yield 10 (42.4 mg; 36.5%); mp 189–191 °C. <sup>1</sup>H NMR (DMSO-*d*<sub>6</sub>) δ 3.21 (t, 4H, piperazine CH<sub>2</sub>), 3.56 and 3.68 (2 × dd, 2H, CH<sub>2</sub>-5'), 3.97 (q, 1H, H-4'), 4.16 (t, 1H, H-2'),

4.38 (br s, 4H, piperazine CH<sub>2</sub>), 4.59 (t, 1H, H-3'), 5.23 (br s, 1H, 3'-OH), 5.48 (br s, 1H, 5'-OH), 5.94 (d, 1H, 1'-H), 7.01–7.10 (m, 4H, H-2,3,5,6 in phenyl), 8.28 (s, 1H, H-8), 8.45 (s, 1H, H-2). <sup>13</sup>C NMR (DMSO-*d*<sub>6</sub>) δ 45.16, 49.96 (CH<sub>2</sub> in piperazine), 62.15 (CH<sub>2</sub>-5'), 71.14 (CH-3'), 74.22 (CH-2'), 86.42 (CH-4'), 88.45 (CH-1'), 115.91, 116.13, 118.37 (2), 120.33 (C in phenyl), 139.67 (C-5), 148.51 (C-8), 150.99 (C-6), 152.47 (C-2), 153.79 (C-4). HRMS (ESI+) *m/z* calcd for C<sub>20</sub>H<sub>24</sub>FN<sub>6</sub>O<sub>4</sub> (M + H)<sup>+</sup> 431.1843, found 431.1846. Anal. Calcd for C<sub>20</sub>H<sub>23</sub>FN<sub>6</sub>O<sub>4</sub>·0.5H<sub>2</sub>O: C, 54.66; H, 5.50; N, 19.12. Found C, 54.62; H, 5.32; N, 19.25.

**6-[4-(4-Trifluoromethylphenyl)piperazine-1-yl]-9-(β-D-ribofuranosyl)-9H-purine (11).** The compound was prepared from (6) (106.4 mg, 0.17 mmol) at room temperature for 1 h according to the general procedure and was purified by column chromatography (EtOAc) to yield **11** (15 mg; 17.8%); mp 108–110 °C. <sup>1</sup>H NMR (DMSO-*d*<sub>6</sub>) δ 3.45 (t, 4H, piperazine CH<sub>2</sub>), 3.52–3.60 and 3.64–3.72 (2*m*, 2H, CH<sub>2</sub>-5'), 3.96–4.17 (m, 2H, H-2', 3'), 4.38 (br s, 4H, piperazine CH<sub>2</sub>), 4.59 (q, 1H, H-4'), 5.21 (d, 1H, 3'-OH), 5.33 (t, 1H, 5'-OH), 5.48 (d, 1H, 2'-OH), 5.93 (d, 1H, 1'-H), 7.14 (d, *J*<sub>o</sub> = 8.8 Hz, 2H, H-2,6), 7.54 (d, *J*<sub>o</sub> = 8.8 Hz, 2H, H-3,5), 8.29 (s, 1H, H-8), 8.46 (s, 1H, H-2). <sup>13</sup>C NMR (DMSO-*d*<sub>6</sub>) δ 44.87, 47.65 (CH<sub>2</sub> in piperazine), 62.15 (CH<sub>2</sub>-5'), 71.14 (CH-3'), 74.24 (CH-2'), 86.42 (CH-4'), 88.46 (CH-1'), 115.06, 118.79 (q), 120.37, 124.29 (C in phenyl), 126.87 (q) (CF<sub>3</sub>), 139.73 (C-5), 151.01 (C-8), 152.48 (C-6), 153.79 (C-2), 153.82 (C-4). HRMS (ESI+) *m/z* calcd for C<sub>21</sub>H<sub>24</sub>F<sub>3</sub>N<sub>6</sub>O<sub>4</sub> (M + H)<sup>+</sup> 481.1811, found 481.1810. Anal. Calcd for C<sub>21</sub>H<sub>23</sub>F<sub>3</sub>N<sub>6</sub>O<sub>4</sub>·0.6H<sub>2</sub>O: C, 51.34; H, 4.96; N, 17.10. Found C, 51.65; H, 4.74; N, 16.73.

**6-[4-(3,4-Dichlorophenyl)piperazine-1-yl]-9-(β-D-ribofuranosyl)-9H-purine (12).** The compound was prepared from (7) (166.2 mg, 0.27 mmol) at room temperature for 12 h according to the general procedure and was purified by column chromatography (EtOAc-hexane,4:1 and then EtOAc) to yield **12** (90 mg; 68.7%); mp 211 °C. <sup>1</sup>H NMR (DMSO-*d*<sub>6</sub>) δ 3.34 (t, 4H, piperazine CH<sub>2</sub>), 3.51–3.60 and 3.65–3.73 (2*m*, 2H, CH<sub>2</sub>-5'), 3.92–4.63 (m, 7H, H-2',3',4', piperazine CH<sub>2</sub>), 5.21 (d, 1H, 3'-OH), 5.33 (t, 1H, 5'-OH), 5.47 (d, 1H, 2'-OH), 5.94 (d, *J* = 5.6 Hz, 1H, 1'-H), 7.00 (d, *J*<sub>o</sub> = 7.2 Hz, 1H, H-6 in phenyl), 7.21 (s, 1H, H-2 in phenyl), 7.29 (d, *J* = 9.2 Hz, 1H, H-5 in phenyl), 8.29 (s, 1H, H-8), 8.45 (s, 1H, H-2). <sup>13</sup>C NMR (DMSO-*d*<sub>6</sub>) δ 29.69 (CH<sub>2</sub> in piperazine), 48.30 (CH<sub>2</sub> in piperazine), 62.18 (CH<sub>2</sub>-5'), 71.16 (CH-3'), 74.25 (CH-2'), 86.44 (CH-4'), 88.47 (CH-1'), 116.26 (CH in phenyl), 117.25 (CH in phenyl), 120.37 (CH in phenyl), 120.60 (C in phenyl), 131.21 (C in phenyl), 132.24 (C in phenyl), 139.76 (C-5), 151.03 (C-8), 151.31 (C-6), 152.50 (C-2), 153.81 (C-4). HRMS (ESI+) *m/z* calcd for C<sub>20</sub>H<sub>23</sub>Cl<sub>2</sub>N<sub>6</sub>O<sub>4</sub> (M)<sup>+</sup> 481.1158, found 481.1156. Anal. Calcd for C<sub>20</sub>H<sub>22</sub>Cl<sub>2</sub>N<sub>6</sub>O<sub>4</sub>·0.2C<sub>6</sub>H<sub>14</sub>: C, 51.07; H, 5.01; N, 16.86. Found C, 51.46; H, 4.88; N, 16.56.

**6-(4-(Diphenylmethyl)piperazine-1-yl)-9-(β-D-ribofuranosyl)-9H-purine (13).** The compound was prepared from (8) (166.8 mg, 0.26 mmol) at room temperature for 8 h according to the general procedure and was purified by column chromatography (EtOAc and then EtOAc-MeOH, 6:1) to yield **13** (60.5 mg; 45.5%); mp 117–119 °C. <sup>1</sup>H NMR (DMSO-*d*<sub>6</sub>) δ 2.43 (br s, 4H, piperazine CH<sub>2</sub>), 3.50–3.58 ve 3.62–3.69 (2*m*, 2H, CH<sub>2</sub>-5'), 3.92–4.38 (m, 7H, piperazine CH<sub>2</sub>, CH, H-2', 3'), 4.55 (q, 1H, H-4'), 5.19 (d, *J* = 4.4 Hz, 1H, 3'-OH), 5.31 (t, *J* = 5.2 Hz, 1H, 5'-OH), 5.46 (d, *J* = 6 Hz, 1H, 2'-OH), 5.90 (d, *J* = 5.6 Hz, 1H, H-1'), 7.21 (t, *J*<sub>o</sub> = 7.2 Hz, 2H, H-4 in phenyl), 7.32 (t, *J*<sub>o</sub> = 7.2 Hz, 4H, H-3,5 in phenyl), 7.45 (d, *J*<sub>o</sub> = 8 Hz, 4H, H-2,6 in phenyl), 8.22 (s, 1H, H-8), 8.39 (s, 1H, H-2). <sup>13</sup>C NMR (DMSO-*d*<sub>6</sub>) δ 52.18 (CH<sub>2</sub> in piperazine), 62.14 (CH), 71.13 (CH<sub>2</sub>-5'), 74.20 (CH-3'), 75.48 (CH-2'), 86.39 (CH-4'), 88.42 (CH-1'), 120.27 (CH in phenyl), 127.65 (CH in phenyl), 128.35 (CH in phenyl), 129.26 (C in phenyl), 139.54 (C-5), 143.12 (C-8), 150.93 (C-6), 152.41 (C-2), 153.82 (C-4). HRMS (ESI+) *m/z* calcd for C<sub>27</sub>H<sub>31</sub>N<sub>6</sub>O<sub>4</sub> (M + H)<sup>+</sup> 503.2407, found 503.2406. Anal. Calcd for C<sub>27</sub>H<sub>30</sub>N<sub>6</sub>O<sub>4</sub>·0.2EtOAc·1.0H<sub>2</sub>O: C, 62.03; H, 6.29; N, 15.61. Found C, 61.72; H, 6.05; N, 15.21.

**Cells and Culture.** The human primary liver cancer cell lines (Huh7, HepG2, Mahlavu, and FOCUS) were grown in Dulbecco's Modified Eagle's Medium (DMEM) (Invitrogen GIBCO), with 10% fetal bovine serum (FBS) (Invitrogen GIBCO), nonessential amino

acids, and 1% penicillin (Biochrome). It was incubated at 37 °C with 5% CO<sub>2</sub>. DMSO (Sigma) was used as a solvent for the compounds. The concentration of DMSO was always less than 1% in the cell culture medium. The cytotoxic drugs (Camptothecin, 5FU, doxorubicin, and MeSAAdo) used as positive controls were from Calbiochem.

**Sulforhodamine B (SRB) Assay for Cytotoxicity Screening.** Huh7, HCT116, MCF7, HepG2, Mahlavu, and FOCUS cells were inoculated (2000–10000 cells/well in 200 μL) in 96-well plates. The next day, the media were refreshed and the compounds dissolved in DMSO were applied in concentrations between 1 and 40 μM in parallel with DMSO-only treated cells as negative controls. At the 72nd hour of treatment with compounds **9–13** and the other drugs, the cancer cells were fixed with 100 μL of 10% (w/v) trichloroacetic acid (TCA) and kept at +4 °C in the dark for one hour. TCA fixation was terminated by washing the wells with ddH<sub>2</sub>O five times. Air-dried plates were stained with 0.4% sulphorhodamine B (SRB) dissolved in 1% acetic acid solution for 10 min in the dark and at room temperature. The protein-bound and dried SRB dye was then solubilized with 10 mM Tris-Base pH 8. The absorbance values were obtained at 515 nm in a microplate reader. The data normalized against DMSO only treated wells, which were used as controls in serial dilutions. In all experiments, a linear response was observed, with serial dilutions of the compounds and the drugs; R<sub>2</sub> ≥ 0.9.

**Real-Time Cell Electronic Sensing (RT-CES) for Cytotoxicity Profiling.** The proliferation of primary liver cancer cell lines was monitored in real-time cell electronic sensing (RT-CES) (xCELLigence-Roche Applied Science), and the cell index (CI) was measured every 30 min for 96 h. Huh7, HepG2, Mahlavu, and FOCUS cells were inoculated (2000 cells/well in 200 μL) in the 96 well E-plate on the xCELLigence station in 5% CO<sub>2</sub> at 37 °C. The CI values were recorded every 30 min. The next day, 150 μL of medium from each well was replaced with 100 μL of fresh medium containing compound **11** applied in the indicated concentrations. The CI values were recorded every 30 min to monitor real-time drug response. DMSO-only and medium-only wells were also included in the monitoring to account for their possible solitary effects on cancer cells.

**Kinase Assay.** Kinase-Glo-Plus luminescence kinase activity assay (Promega) was performed according to the manufacturer's protocol. First, the Kinase-Glo reaction buffer (40 mM Tris-HCl pH7.6, 20 mM MgCl<sub>2</sub>, 0.1 mg/mL BSA) was placed in the wells of a 96-well Elisa plate. Then, Huh7 cells treated with **11**, Staurosporin (STS), and MeSAAdo for 72 h. Next, lysates from 80000 cells were placed into the wells. DMSO used as negative control. The total volume of the lysates and the kinase reaction buffer was 50 μL. Then, 50 μL of Kinase-Glo reagent (Kinase-Glo plus substrate + Kinase-Glo-Plus buffer) was applied. After 10 min of dark incubation at room temperature, the luminescence was detected with a luminometer. If kinase activity is diminished, ATP concentration will increase and so will luminescence.

**Senescence Associated-β-gal Assay and BrdU Proliferation Co-staining.** Huh7 cells (5000cell) were inoculated in two identical six-well plates on coverslips. The next day, compound **11** and doxorubicin at the indicated concentrations, and their corresponding DMSO controls were applied to the plates. On day three and the day six, the senescence-associated-β-gal (SAβgal) assay and BrdU containing were performed as described previously.<sup>23,24</sup>

**Western Blot Analysis.** Proteins from Huh7 cells treated with compound **11** and doxorubicin for three and six days were separated on a 10% SDS-PAGE, transferred onto nitrocellulose membranes, and visualized, as described previously.<sup>19</sup> The total homogenates from the cells were resuspended in 50 mM Tris-HCl pH 7.4, 1 mM EDTA, 1 mM EGTA, 150 mM NaCl, 1% Triton X-100, and 0.1% SDS with a protease-inhibitor cocktail and phosphatase inhibitors. p15, Rb and pRb were detected by Western blotting. Actin protein was used for equal loading control.

## ■ AUTHOR INFORMATION

### Corresponding Author

\*For M.T.: phone, +90 312 203 3071; fax, +90 312 213 1081; E-mail, tuncbile@pharmacy.ankara.edu.tr. For R.C.A.: phone,

+90 312 290 2503; fax, +90 312 266 5097; E-mail: rengul@bilkent.edu.tr.

### Notes

The authors declare no competing financial interest.

### ACKNOWLEDGMENTS

This work was supported by the Scientific and Technological Research Council of Turkey-TUBITAK (TBAG-109T987), the KANILTEK Project from the State Planning Organization of Turkey (DPT), and Bilkent University funds. We thank to Professor Hakan Goker and Dr. Mehmet Alp from Central Instrumentation Laboratory of Faculty of Pharmacy, Ankara University for NMR and elemental analyses and to Dr. Murat K. Sukuroglu from Faculty of Pharmacy, Gazi University for HRMS. We thank R. Nelson for editing the English of the final version of our manuscript.

### REFERENCES

- (1) Karran, P. Thiopurines, DNA damage, DNA repair and therapy-related cancer. *Br. Med. Bull.* **2006**, *79*–80, 153–170.
- (2) Bosch, L.; Harbers, E.; Heidelberger, C. Studies on fluorinated pyrimidines. V. Effects on nucleic acid metabolism in vitro. *Cancer Res.* **1958**, *18*, 335–343.
- (3) Sampath, D.; Rao, V. A.; Plunkett, W. Mechanisms of apoptosis induction by nucleoside analogs. *Oncogene* **2003**, *22*, 9063–9074.
- (4) Escherich, G.; Richards, S.; Stork, L. C.; Vora, A. J. Childhood Acute Lymphoblastic Leukaemia Collaborative Group (CALLCG). Meta-analysis of randomised trials comparing thiopurines in childhood acute lymphoblastic leukaemia. *Leukemia* **2011**, *25*, 953–959.
- (5) Lech-Maranda, E.; Korycka, A.; Robak, T. Meta-analysis of randomised trials comparing thiopurines in childhood acute lymphoblastic leukaemia. *Mini-Rev. Med. Chem.* **2006**, *6*, 575–581.
- (6) Wilson, P. K.; Mulligan, S. P.; Christopherson, R. I. Metabolic response patterns of nucleotides in B-cell chronic lymphocytic leukaemias to cladribine, fludarabine and deoxycoformycin. *Leukemia Res.* **2004**, *28*, 725–731.
- (7) Nakamura, J.; Kohya, N.; Kai, K.; Ohtaka, K.; Hashiguchi, K.; Hiraki, M.; Kitajima, Y.; Tokunaga, O.; Noshiro, H.; Miyazaki, K. Ribonucleotide reductase subunit M1 assessed by quantitative double-fluorescence immunohistochemistry predicts the efficacy of gemcitabine in biliary tract carcinoma. *Int. J. Oncol.* **2010**, *37*, 845–852.
- (8) Simon, G. R.; Schell, M. J.; Begum, M.; Kim, J.; Chiappori, A.; Haura, E.; Antonia, S.; Beppler, G. Preliminary indication of survival benefit from ERCC1 and RRM1-tailored chemotherapy in patients with advanced nonsmall cell lung cancer: Evidence from an individual patient analysis. *Cancer* **2011**, Oct 25, Epub (DOI: 10.1002/cncr.26522).
- (9) Dick, J.; Wright, J. On the importance of deoxyribonucleotide pools in the senescence of cultured human diploid fibroblasts. *FEBS Lett.* **1985**, *179*, 21–24.
- (10) Ricci, M. S.; Zong, W.-X. Chemotherapeutic approaches for targeting cell death pathways. *Oncologist* **2006**, *11*, 342–357.
- (11) Harley, C. B.; Futcher, A. B.; Greider, C. W. Telomeres shorten during ageing of human fibroblasts. *Nature* **1990**, *345*, 458–460.
- (12) Collado, M.; Serrano, M. The power and the promise of oncogene-induced senescence markers. *Nature Rev. Cancer* **2006**, *6*, 472–476.
- (13) Serrano, M.; Lin, A. W.; McCurrach, M. E.; Beach, D.; Lowe, S. W. Oncogenic ras provokes premature cell senescence associated with accumulation of p53 and p16INK4a. *Cell* **1997**, *88*, 593–602.
- (14) Nardella, C.; Clohessy, J. G.; Alimonti, A.; Pandolfi, P. P. Pro-senescence therapy for cancer treatment. *Nature Rev. Cancer* **2011**, *11*, 503–511.
- (15) Kang, T.-W.; Yevsa, T.; Woller, N.; Hoenicke, L.; Wuestefeld, T.; Dauch, D.; Hohmeyer, A.; Gereke, M.; Rudalska, R.; Potapova, A.; Iken, M.; Vucur, M.; Weiss, S.; Heikenwalder, M.; Khan, S.; Gil, J.; Bruder, D.; Manns, M.; Schirmacher, P.; Tacke, F.; Ott, M.; Luedde,

T.; Longerich, T.; Kubicka, S.; Zender, L. Pro-senescence therapy for cancer treatment. *Nature* **2011**, *479*, 547–551.

(16) Irmak, M. B.; Ince, G.; Ozturk, M.; Cetin-Atalay, R. Acquired tolerance of hepatocellular carcinoma cells to selenium deficiency: a selective survival mechanism? *Cancer Res.* **2003**, *63*, 6707–6715.

(17) Finn, R. S. Sorafenib use while waiting for liver transplant: We still need to wait. *J. Hepatol.* **2012**, *56*, 723–725.

(18) Andrzejewska, M.; Kamiński, J.; Kazimierzczuk, Z. Microwave induced synthesis of ribonucleosides on solid support. *Nucleosides, Nucleotides, Nucleic Acids* **2002**, *21*, 73–78.

(19) Buontempo, F.; Ersahin, T.; Missirolì, S.; Senturk, S.; Etro, D.; Ozturk, M.; Capitani, S.; Cetin-Atalay, R.; Neri, M. L. Inhibition of Akt signaling in hepatoma cells induces apoptotic cell death independent of Akt activation status. *Invest. New Drugs* **2011**, *29*, 1303–1313.

(20) Gobeil, S.; Boucher, C. C.; Nadeau, D.; Poirier, G. G. Characterization of the necrotic cleavage of poly(ADP-ribose) polymerase (PARP-1): implication of lysosomal proteases. *Cell Death Differ.* **2001**, *8*, 588–594.

(21) Shay, J. W.; Roninson, I. B. Hallmarks of senescence in carcinogenesis and cancer therapy. *Oncogene* **2004**, *23*, 2919–2933.

(22) Hanahan, D.; Weinberg, R. A. Hallmarks of cancer: the next generation. *Cell* **2011**, *144*, 646–674.

(23) Dimri, G. P.; Lee, X.; Basile, G.; Acosta, M.; Scott, G.; Roskelley, C.; Medrano, E. E.; Linskens, M.; Rubelj, I.; Pereira-Smith, O. A biomarker that identifies senescent human cells in culture and in aging skin in vivo. *Proc. Natl. Acad. of Sci. U.S.A.* **1995**, *92*, 9363–9367.

(24) Ozturk, N.; Erdal, E.; Mumcuoglu, M.; Akcali, K. C.; Yalcin, O.; Senturk, S.; Arslan-Ergul, A.; Gur, B.; Yulug, I.; Cetin-Atalay, R.; Yakicier, C.; Yagci, T.; Tez, M.; Ozturk, M. Reprogramming of replicative senescence in hepatocellular carcinoma-derived cells. *Proc. Natl. Acad. of Sci. U.S.A.* **2006**, *103*, 2178–2183.